

# A Note on Decoding Order in User Grouping and Power Optimization for Multi-Cell NOMA with Load Coupling

Lei You and Di Yuan

Department of Information Technology, Uppsala University, Sweden  
{lei.you; di.yuan}@it.uu.se

**Abstract**—In this technical note, we present a new theoretical result for multi-cell non-orthogonal multiple access (NOMA). For multi-cell scenarios, a so-called load-coupling model has been proposed earlier to characterize the presence of mutual interference for NOMA, and the optimization process relies on the use of fixed-point iterations [1], [2] across cells. One difficulty here is that the order of decoding for successive interference cancellation (SIC) in NOMA is generally not known a priori. This is because the decoding order in one cell depends on interference, which, in turn, is governed by resource usage in other cells, and vice versa. To achieve convergence, previous works have used workarounds that pose restrictions to NOMA, such that the SIC decoding order remains throughout the fixed-point iterations. As a comment to [1], [2], we derive and prove the following result: The convergence is guaranteed, even if the order changes over the iterations. The result not only waives the need of previous workarounds, but also implies that a wide class of optimization problems for multi-cell NOMA is tractable, as long as that for single cell is.

**Index Terms**—SIC, NOMA, interference, multi-cell

## I. INTRODUCTION

NON-ORTHOGONAL Multiple Access (NOMA) with successive interference cancellation (SIC) allows more than one user to share resource in the time-frequency domain. With superposition coding, some users may perform SIC to remove (some of) the intra-cell interference. The decoding needs to follow signal strength so as to make SIC succeed. In the simplest case, the decoding order is determined by the channel gains of users. NOMA in single-cell scenarios has been widely addressed [3]–[9]. In multi-cell NOMA, inter-cell interference has an influence on the decoding order, which has to be accounted for [10], [11]. Besides, NOMA requires *user grouping* for resource sharing. The candidate options for user grouping is exponential in the number of users. Third, power allocation (a.k.a *power split*) affects the performance. Both user grouping and power split are intertwined with the decoding order.

The decoding order in one cell depends on the interference from other cells; the interference, in turn, depends on the allocated power and time-frequency resources. Increasing the resource consumption for data transmission in one cell implies more interference to the users located in other cells. One approach for multi-cell optimization for orthogonal multiple access (OMA) consists of fixed point iterations for the so-called *load coupling* equation system [12]–[34]. In every

iteration, the resource allocation of one cells is computed, with the allocation in other cells temporarily being fixed. At convergence, an equilibrium with respect to resource allocation and the resulting interference is obtained. However, in NOMA, applying the type of iterative method is challenging, since the decoding order is not known beforehand, but subject to change during the iterative process. Some references [35]–[39] do not explicitly address the interaction between decoding order and interference. To the best of our knowledge, [1], [2], [40] consider this type of dependency in multi-cell NOMA. In [40], the authors investigate multi-cell NOMA power control without user grouping. References [1], [2] have used workarounds such that some pre-computed decoding order remains NOMA-compliant in optimization, which, on the other hand, poses limitations to the applicable scenarios. To be specific, [40] requires that there is only one candidate group consisting of all users, and [1], [2] require: 1) there are up to two users in each group and 2) the candidate groups are selected such that the NOMA-compliant decoding order can be pre-determined no matter the interference. Without these conditions, neither the convergence nor the optimality of their proposed algorithm is guaranteed.

This technical note serves as a comment to [1], [2], though our main results are not necessarily bound to the specific system setups in [1] and [2]. The contributions are:

- We show a general conclusion with respect to the formulation of multi-cell NOMA optimization problems, such that the decoding order needs not to be explicitly ensured by constraints.
- We use a so-called load-coupling model as an example, to showcase our conclusion. The load coupling model has been widely adopted in OMA scenarios [12]–[34] and has been extended to NOMA in [1], [2].
- We formally proved that, the convergence and the optimality are guaranteed without imposing the limitations on the candidate user groups, even if the decoding order, due to variable inter-cell interference, changes from one iteration to the next in a fixed-point method. Furthermore, the result implies that a wide class of optimization problems for multi-cell NOMA is tractable as long as that for single cell is.

We clarify that in this technical note, the term “*correct decoding order*”, unless otherwise stated, always refers to

the NOMA-compliant decoding order. That is a receiver decodes the signals successively in descending order of signal strengths. This decoding order in NOMA is based on the (valid) assumption that a user with better channel condition (strong user) is able to decode the signal transmitted to another user located in the same cell with worse channel condition (weak user), as long as the weak user can decode the signal of its own. In other words, the data rate encoded in the signal to the weak user is permitted by the signal-to-interference-and-noise ratio (SINR) of the weak user. Since the strong user can receive the signal intended for the weak user better than the weak user itself, the strong user can decode this signal as well, as the weak user can do it (see, e.g., [41], Chapter 6.2.2, pp. 279 for further details).

Following up the above discussion, we remark that it is possible to intentionally lower the rate transmitted to a user, in particular a strong user, such that other, weak users can decode that signal and perform interference cancellation. Such schemes have been studied in, for example, [42], [43]. However, to our knowledge, the literature of NOMA assume that the rate is set to what is maximumly permitted by the SINR, which is the assumption in the current note as well.

## II. SYSTEM MODEL

### A. Preliminaries

Denote by  $\mathcal{I} = \{1, 2, \dots, n\}$  the set of cells, and  $\mathcal{J}$  the set of user equipments (UEs). We consider downlink and use  $g_{ij}$  to denote the gain from cell  $i$  to UE  $j$ . For each cell  $i$  ( $i \in \mathcal{I}$ ), denote by  $\mathcal{J}_i$  the set of UEs located in the cell. Denote by  $d_j$  the data demand of UE  $j$  ( $j \in \mathcal{J}$ ). Denote by  $p_i$  the transmission power of cell  $i$  on each resource unit (RU). By using SIC, multiple UEs of a cell can access one RU simultaneously, with  $p_i$  split among these UEs. We refer to the UEs sharing the same RUs as a *group*, and the process of selecting UEs to form groups as *user grouping*. We use  $u$  to refer to a generic group. For any UE  $j \in u$ , denote by  $q_{ju}$  the portion of power  $p_i$  used for UE  $j$  on each RU used by group  $u$ . For cell  $i$  ( $i \in \mathcal{I}$ ), denote by  $\mathcal{U}_i$  the set of all groups of UEs in  $\mathcal{J}_i$ . In analogy with this, we use  $\mathcal{U}_j$  to refer to the set of all groups that UE  $j$  belongs to. In order to keep generality, we allow also singleton group  $u$ . In this case, the UE in the group does not share RU with others (and hence no SIC), i.e., the UE is in OMA. Besides, we allow one UE to belong to one or multiple groups such that groups may have overlapping UEs. There is no limitation on the number of UEs in one group. Both power split and user grouping are subject to optimization.

In our derivations of the theoretical results, the channel information is known. This is justified in research addressing the achievable performance of a system. In our case, we target providing theoretical results that are useful for computing the optimal performance of NOMA, achieved with known channel information, and thereby assessing accurately the potential benefit of NOMA in comparison to OMA. In practice, imperfect channel estimation will impact of the SIC performance, even though SIC is more robust than parallel interference cancellation (PIC) against error propagation [44]. Moreover,

we remark that there are several schemes for mitigating the issue of propagation error for SIC, including soft-in soft-out (SISO) decoding [44], ordered SIC [45], and multi-feedback and multi-branch SIC [46], [47].

### B. NOMA with SIC

In the following, we consider a generic UE  $j$  located in cell  $i$ , i.e.,  $j \in \mathcal{J}_i$ . The signal-to-interference-and-noise ratio (SINR) of UE  $j$  in group  $u$ , denoted by  $\gamma_{ju}$ , is given below.

$$\gamma_{ju} = \frac{q_{ju}g_{ij}}{\underbrace{\sum_{h \in u} q_{hu}g_{ij}\theta_{hj}}_{\text{intra-cell}} + \underbrace{\sum_{k \in \mathcal{I} \setminus \{i\}} p_k g_{kj} \rho_k}_{\text{inter-cell}} + \sigma^2}, \quad \begin{matrix} j \in u \\ u \in \mathcal{U}_i \end{matrix} \quad (1)$$

The denominator of  $\gamma_{ju}$  consists of three parts: intra-cell interference, inter-cell interference, and noise power  $\sigma^2$ . The optimization variables are the power split  $q_{ju}$ , the decoding order indicator  $\theta_{hj}$  (discussed below), and the cell-level resource allocation  $\rho_k$  that is used as a scaling parameter for the inter-cell interference (discussed below in Section II-C). For each group  $u$ , note that a UE  $j$  of this group decodes the data of UEs with stronger signal in  $u$ , and the signals transmitted to other UEs of  $u$  constitute interference at  $j$ . We use  $\theta_{hj}$  as a binary indicator:  $\theta_{hj} = 1$  if and only if the signal transmission to UE  $h$  is interference to UE  $j$ , and  $\theta_{hj} = 0$  if and only if UE  $j$  can decode the signal of UE  $h$ . As a convention,  $\theta_{hj} = 0$  if  $h = j$ . We remark that  $\theta_{hj}$  is subject to the correct decoding order, which is determined by the channel condition [41]. For any UE  $j$ , define

$$w_j = \left( \sum_{k \in \mathcal{I} \setminus \{i\}} p_k g_{kj} \rho_k + \sigma^2 \right) / g_{ij}. \quad (2)$$

For any user  $j$ , entity  $w_j$  is the amount of inter-cell interference and noise in relation to  $j$ 's own signal gain. Hence a higher value of this entity means poorer channel condition. For two users  $h$  and  $j$  of the same cell,  $h$  is the strong user if  $w_h \leq w_j$ . Recall that, in NOMA, a strong user can decode the signal of a weak user, as long as the weak user can decode the signal (of which the rate is set to be that permitted by the weak user's SINR). Thus,  $\theta_{hj} = 1$  if and only if  $w_h \leq w_j$ , i.e., UE  $h$  has better channel condition than UE  $j$ . We remark that in [41], SIC is discussed for users of a single cell. The result remains applicable here, because even if our scenario consists in multiple cells, NOMA with SIC is used for each individual cell, whereas inter-cell interference is treated in the same way as noise. In addition, as remarked earlier, same as in [41], rate adaptation is not present in NOMA.

In case  $w_h = w_j$ , we assume there is a pre-defined convention to break the tie. One possibility is to follow user index, e.g.,  $\theta_{hj} = 1$  if  $w_h = w_j$  and  $h < j$ . As a result, for given inter-cell interference, the NOMA decoding order is unique.

### C. Cell Load Coupling

We define  $c_{ju}$  as the achievable capacity for UE  $j$  in group  $u$  on one RU, namely,

$$c_{ju} = \log(1 + \gamma_{ju}) = \log\left(1 + \frac{q_{ju}}{\sum_{h \in u} q_{hu} \theta_{hj} + w_j}\right). \quad (3)$$

To ease the presentation of the mathematical proofs, in the theoretical derivations we use the natural logarithm, and hence the information unit is nat [48] rather than bit. Thus, to be consistent, the data demand  $d_j, j \in \mathcal{J}$ , are given in nats.

The load coupling model defines  $\rho_i$  to be the load of cell  $i$ , which is the proportion of cell  $i$ 's time-frequency resource that have been allocated for data transmission. Denote by  $x_u$  the proportion of RUs allocated to group  $u$ . We have  $\rho_i = \sum_{u \in \mathcal{U}_i} x_u$ . From an interference point of view, higher  $\rho_i$  means that cell  $i$  generates more interference to others, hence cell load has been used as an interference scaling parameter [1], [2], [12]–[34], see (1). We remark that, by (2), for any UE  $j$  in cell  $i$ ,  $w_j$  changes with other cells' resource allocation  $\rho_k$  ( $k \in \mathcal{I} \setminus \{i\}$ ). Hence the decoding order depends on the network-wide resource allocation.

We use  $M$  and  $B$  to represent the total number of RUs in one cell and the bandwidth of each RU, respectively. To satisfy UE  $j$ 's demand  $d_j$ , we have

$$\sum_{u \in \mathcal{U}_j} M B c_{ju} x_u \geq d_j, j \in \mathcal{J}, \quad (4)$$

imposing that  $d_j$  is satisfied by the sum of the demand delivered to UE  $j$  over all groups in  $\mathcal{U}_j$ . In the discussion below, we use normalized  $d_j$  such that the notation  $M$  and  $B$  are not necessary in our presentation.

## III. PROBLEM FORMULATION

### A. Mathematical Formulation

We consider UE grouping and power split in NOMA, subject to inter-cell interference that is modelled using the load-coupling model, as outlined in the previous section. The cost function is defined with respect to the amount of RUs needed to meet the user demand, i.e., cell load as defined earlier. More specifically, we address power split  $\mathbf{q}$ , group-level resource allocation  $\mathbf{x}$ , and cell-level resource allocation  $\boldsymbol{\rho}$ . Moreover, as mentioned in Section II-B,  $\boldsymbol{\theta}$  is the decoding order indicator that in turn depends on cell load. The objective function  $F$  is a generic cost function of the cell loads (i.e. time-frequency resource usage of cells) and  $F$  is monotonically increasing in  $\rho_1, \rho_2, \dots, \rho_n$  element-wisely. The optimization formulation is given in (5) below. Note that in the formulation, the rate of a UE equals what is permitted by the SINR, where  $\boldsymbol{\theta}$  is present for modeling intra-cell interference. In other words, rate adaptation/optimization in SIC is not part of the model.

The user demand constraints are (5b) and (5c)<sup>1</sup>. Constraints (5d) impose the power limit, and equations (5e) define cell load. Constraints (5f)–(5h) are for the decoding order.

<sup>1</sup>With  $d_j$  being normalized by  $M \times B$  in this formulation, one can refer to (1) and (2) to verify that constraints (5b) along with (5c) are equivalent to (4) in Section II-C.

$$\min_{\substack{\mathbf{q}, \mathbf{x}, \boldsymbol{\rho}, \mathbf{w} \geq \mathbf{0} \\ \boldsymbol{\theta} \in \{0,1\}}} F(\rho_1, \rho_2, \dots, \rho_n) \quad (5a)$$

$$\text{s.t.} \quad \sum_{u \in \mathcal{U}_j} \log\left(1 + \frac{q_{ju}}{\sum_{h \in u} q_{hu} \theta_{hj} + w_j}\right) x_u \geq d_j, j \in \mathcal{J} \quad (5b)$$

$$w_j = \frac{\sum_{k \in \mathcal{I} \setminus \{i\}} p_k g_{kj} \rho_k + \sigma^2}{g_{ij}}, j \in \mathcal{J}_i, i \in \mathcal{I} \quad (5c)$$

$$\sum_{j \in u} q_{ju} \leq p_i, u \in \mathcal{U}_i, i \in \mathcal{I} \quad (5d)$$

$$\rho_i = \sum_{u \in \mathcal{U}_i} x_u, i \in \mathcal{I} \quad (5e)$$

$$w_j > w_h \vee (w_j = w_h \wedge h < j) \Rightarrow \theta_{hj} = 1, \\ h \neq j, h, j \in u, u \in \mathcal{U}_i, i \in \mathcal{I} \quad (5f)$$

$$\theta_{hj} + \theta_{jh} = 1, h \neq j, h, j \in u, u \in \mathcal{U}_i, i \in \mathcal{I} \quad (5g)$$

$$\theta_{hj} \in \{0, 1\}, h \neq j, h, j \in u, u \in \mathcal{U}_i, i \in \mathcal{I} \quad (5h)$$

Specifically, we have  $\theta_{hj} = 1$  if  $w_h < w_j$  or if  $h < j$  in case of a tie, otherwise  $\theta_{hj} = 0$ , following the rule of the correct decoding order in Section II-B. Note that the decoding order depends on the cell level resource allocation, i.e.,  $\rho_1, \rho_2, \dots, \rho_n$ . Moreover, as will be clear later, stating (5f) in logic form does not have any impact on the theoretical results.

We remark that in reality there is an upper limit  $\bar{\rho}$  for cell load, with the constraint  $\rho_i \leq \bar{\rho}, i \in \mathcal{I}$ . As will be shown later, this constraint can be accounted for in post-processing. Moreover, if necessary, user group selection constraints can be added to (5), and our conclusion in this paper still holds.

### B. Obstacles of Solving (5)

We remark that (5) is highly non-linear. In addition, a major obstacle for some iterative algorithms for (5) is that, the variation of resource allocation in each iteration leads to the change of decoding order for each group. There is an algorithmic framework derived in [1], [2], which uses a top-down paradigm (detailed in Section III-C). The basic idea is to break down (5) into single cell level and then solve the single-cell problems iteratively. For each iteration, there is an inner loop over the cells. This inner loop can be performed in parallel or sequentially. In the former case, the optimized resource allocation of all cells serves as the input of the next iteration. In the latter case, the optimized resource allocation of one cell updates this cell's interference in the input, when the subproblem of another cell is solved. Then, by fixed-point theory, the authors proved the convergence of the algorithm, as well as the optimality of the solution at convergence.

However, the algorithmic framework relies on two restrictions of candidate groups, see [1, Lemma 1] and [2, Lemma 1], respectively: Only those groups of which the decoding orders can be pre-determined, are considered for optimization. The other groups are eliminated from  $\mathcal{U}$ . The limitation states that the decoding orders of all the candidate groups must be

independent of the inter-cell interference such that the orders remain correct all the time, resulting in sub-optimality. To have a high probability of forming such groups, [1, Lemma 1] and [2, Lemma 1] require each group to consist of up to two UEs.

(*Open Problem*) We remark that, if the restrictions are dropped, then in each iteration, the variation of cell loads may lead to the change of decoding order. In this case, neither convergence nor optimality is known.

### C. Solution of [1], [2] for (5)

By considering only groups for which the decoding order is independent of interference, the variable  $\theta$  along with (5f)–(5h) can be dropped from (5), since  $\theta$  is pre-determined in this special case. The algorithmic framework in [1], [2] is detailed as follows. Consider any cell  $i$ , one can define the single-cell load minimization problem as a function of the other cells' loads  $\rho_{-i} = [\rho_1, \rho_2, \dots, \rho_{i-1}, \rho_{i+1}, \dots, \rho_n]$ , denoted by  $\phi_i$ :

$$\phi_i(\rho_{-i}) = \min_{\rho_i, \mathbf{x}, \mathbf{w}} \rho_i \text{ s.t. (5b)–(5e) of cell } i \quad (6)$$

The authors proved that solving (5) amounts to obtaining the fixed point of vector of functions  $\phi = [\phi_1, \phi_2, \dots, \phi_n]$ , that is, to solve  $\rho = \phi(\rho)$ . To be specific, the authors first proved that  $\phi_i$  ( $i \in \mathcal{I}$ ) is a standard interference function (SIF) [49], of which the definition is given below.

**Definition 1.** Any function  $\phi(\rho)$  that has the following two properties is an SIF, where  $\rho$  and  $\rho'$  are two arbitrary non-negative vectors with  $\rho \geq \rho'$ .

- 1) (*Scalability*)  $\alpha\phi(\rho) > \phi(\alpha\rho)$  for any  $\alpha > 1$ .
- 2) (*Monotonicity*)  $\phi(\rho) \geq \phi(\rho')$ .

Based on the fact that  $\phi_i(\rho_{-i})$  ( $i \in \mathcal{I}$ ) is SIF, one can obtain the unique fixed point  $\rho^*$  with  $\rho^* = \phi(\rho^*)$ , by fixed-point iterations on  $\phi$  [49]. Namely, for the iterative process  $\rho^{(k+1)} = \phi(\rho^{(k)})$  ( $k \geq 0$ ), we have  $\lim_{k \rightarrow \infty} \rho^{(k)} = \rho^*$ , for arbitrary non-negative starting point  $\rho^{(0)}$ . At convergence of the fixed-point iterations,  $\rho^*$  along with the other variables  $\mathbf{q}, \mathbf{x}, \mathbf{w}$  that are obtained by solving (6) at  $\rho_{-i}^*$  for all  $i \in \mathcal{I}$ , is optimal to (5).

## IV. RESULTS

This section derives our theoretical results, which give the answer to the open problem in Section III. Our main conclusion is that [1, Lemma 1] and [2, Lemma 1] can be dropped, without loss of optimality or convergence of the proposed solution methods. To show this, we first prove a general conclusion in Section IV-A that is not tied to the load coupling system. The conclusion states that, even if algebraically one allows the capacity formula  $c_{ju} = \log(1 + \gamma_{ju})$  with “decoding orders” in  $u$  to be all possible permutations of UEs of the group, the correct decoding order leads to the largest  $c_{ju}$ . Based on this, we prove in Section IV-B the convergence of the solution methods. We then show the optimality after the convergence proof.

### A. Pseudo Rate Region

Consider *rate region* at the RU level. For a generic cell and a user group  $u$  under consideration, we use  $\theta^*$  to refer to the correct decoding order, i.e., the decoding order used by NOMA for the users in  $u$ . Note that  $\theta^*$  differs by user group, and for a given group,  $\theta^*$  will change from one iteration to another, when applying fixed-point iterations in solving (5). However, within any iteration, when considering a specific group, the amount of interference is given, and hence  $\theta^*$  is easily determined as below, where entities  $w_h$  and  $w_j$  contain the interference terms. For readability, we do not put cell, group, or iteration index on  $\theta^*$ .

$\theta_{hj}^* = 1$  iff  $w_j > w_h$  or ( $w_j = w_h$  and  $h < j$ ),  $h \neq j, h, j \in u$ .

Suppose there are  $K$  ( $K \geq 2$ ) UEs multiplexed on an RU. The UEs are now indexed by following the correct decoding order as defined above. That is, UE 1 decodes UEs 2,  $\dots$ ,  $K$ . UE 2 has the signal intended for UE 1 as interference, and decodes UEs 3,  $\dots$ ,  $K$ , and so on. The capacity of UE  $j$  ( $j = 1, 2, \dots, K$ ), denoted by  $c_j$ , is

$$c_j = \log \left( 1 + \frac{q_j}{\sum_{h=1}^{j-1} q_h + w_j} \right).$$

Considering RU power limit  $p$ , the power split constraint reads

$$\sum_{j=1}^K q_j \leq p. \quad (7)$$

The rates of UEs 1, 2,  $\dots$ ,  $K$  are as follows.

$$\begin{aligned} c_1 &= \log \left( 1 + \frac{q_1}{w_1} \right) \\ c_2 &= \log \left( 1 + \frac{q_2}{q_1 + w_2} \right) \\ &\vdots \\ c_K &= \log \left( 1 + \frac{q_K}{\sum_{h=1}^{K-1} q_h + w_K} \right) \end{aligned}$$

For UE 1, we have

$$c_1 = \log \left( 1 + \frac{q_1}{w_1} \right) \Rightarrow q_1 = w_1 e^{c_1} - w_1$$

For UE 2, we have

$$\begin{aligned} c_2 &= \log \left( 1 + \frac{q_2}{q_1 + w_2} \right) \\ &\Rightarrow q_1 + q_2 = w_1 e^{c_1 + c_2} + (w_2 - w_1) e^{c_2} - w_2 \end{aligned}$$

By successively applying the same formula until the last user  $K$ , we obtain the equation below, where  $w_0 = 0$ .

$$R_{\theta^*}(\mathbf{c}) = \sum_{j \in u} q_{ju} = \sum_{t=1}^K (w_t - w_{t-1}) e^{\sum_{k=t}^K c_k} - w_K \quad (8)$$

where  $\mathbf{c} = [c_1, c_2, \dots, c_K]$ , and  $\boldsymbol{\theta}^*$  indicates the correct decoding order. Consequently, the power split constraint (7) is equivalent to the inequality below

$$R_{\boldsymbol{\theta}^*}(\mathbf{c}) \leq p, \quad (9)$$

where the power split variables  $q_1, q_2, \dots, q_j$  are replaced by variables  $c_1, c_2, \dots, c_K$  that represent the rates, respectively for UEs  $1, 2, \dots, K$ . Inequality (9) forms a bounded area and is the *rate region* of all the  $K$  UEs.

We remark that though the discussion above is based on applying the successive rule on UEs by following their correct decoding order, the rule is also applicable for the case that UEs are ordered arbitrarily. Namely, for a group of UEs that are indexed in any given permutation of the UEs, this successive rule also gives a formula with the same form as (8). We introduce notations to represent this formula in general. Define by  $\mathcal{T}$  the index set of the  $K!$  permutations of the  $K$  UEs. For permutation  $t \in \mathcal{T}$ ,  $\pi_t(j)$  is the position of UE  $j$  in the permutation. Define  $\mathcal{B}$  as a domain of  $\boldsymbol{\theta}$ , derived for all the permutations, i.e.,

$$\mathcal{B} = \{\boldsymbol{\theta} : \theta_{h_j} = 1 \text{ iff } \pi_t(h) < \pi_t(j), t \in \mathcal{T}\}.$$

We use  $R_{\boldsymbol{\theta}}$  as a generic notation to represent (8) defined for the order indicated by  $\boldsymbol{\theta}$  ( $\boldsymbol{\theta} \in \mathcal{B}$ ), so as to distinguish from the formula  $R_{\boldsymbol{\theta}^*}$  that is specified for the correct decoding order.

We name the region defined by  $R_{\boldsymbol{\theta}}(\mathbf{c}) \leq p^{\max}$  with any  $\boldsymbol{\theta} \in \mathcal{B}$  as *pseudo rate region*.

$$R_{\boldsymbol{\theta}}(\mathbf{c}) \leq p, \quad \boldsymbol{\theta} \in \mathcal{B} \quad (10)$$

The reason for the name ‘‘pseudo’’ is because, with  $\boldsymbol{\theta}$  ( $\boldsymbol{\theta} \neq \boldsymbol{\theta}^*$ ), the SIC may not be successfully performed for all UEs.

**Theorem 1.** *Any pseudo rate region is a subset of the rate region of the correct decoding order. Namely,*

$$\{\mathbf{c} : R_{\boldsymbol{\theta}}(\mathbf{c}) \leq p\} \subseteq \{\mathbf{c} : R_{\boldsymbol{\theta}^*}(\mathbf{c}) \leq p\}$$

or equivalently,

$$R_{\boldsymbol{\theta}^*}(\mathbf{c}) \leq R_{\boldsymbol{\theta}}(\mathbf{c}), \text{ for any } \mathbf{c} \geq \mathbf{0}$$

holds for any  $\boldsymbol{\theta} \in \mathcal{B}$ .

*Proof.* Consider the pseudo rate region for  $\boldsymbol{\theta}$  ( $\boldsymbol{\theta} \in \mathcal{B}$ ), i.e.  $R_{\boldsymbol{\theta}}(\mathbf{c}) \leq p$ . We index the UEs from 1 to  $K$  by following the order indicated by  $\boldsymbol{\theta}$ . We remark that if  $\boldsymbol{\theta}$  is not the correct decoding order (i.e.  $\boldsymbol{\theta} \neq \boldsymbol{\theta}^*$ ), then there must exist two UEs that are adjacent in the list, denoted by  $\ell$  and  $\ell + 1$ , such that  $w_{\ell} > w_{\ell+1}$ . We swap the order of the two, and denote by  $\boldsymbol{\theta}'$  the new decoding order. Below, we prove  $R_{\boldsymbol{\theta}'}(\mathbf{c}) \leq R_{\boldsymbol{\theta}}(\mathbf{c})$  for any non-negative  $\mathbf{c}$ .

To ease our representation, we define  $w_0 = 0$  and  $w_{K+1} = w_{K+2}$ . We also explicitly impose that for any summation notation ‘‘ $\sum_{t=a}^b$ ’’ in our expression, if  $b < a$ , then this term in the sum equals zero.

For  $\ell$  and  $\ell + 1$  ( $\ell = 1, 2, \dots, K - 1$ ), we have

$$\begin{aligned} R_{\boldsymbol{\theta}}(\mathbf{c}) &= \sum_{t=1}^{\ell-1} (w_t - w_{t-1}) e^{\sum_{k=t}^K c_k} \\ &\quad + (w_{\ell} - w_{\ell-1}) e^{\sum_{k=\ell}^K c_k} \\ &\quad + (w_{\ell+1} - w_{\ell}) e^{c_{\ell} + \sum_{k=\ell+2}^K c_k} \\ &\quad + (w_{\ell+2} - w_{\ell+1}) e^{\sum_{k=\ell+2}^K c_k} \\ &\quad + \sum_{t=\ell+2}^K (w_{t+1} - w_t) e^{\sum_{k=t+1}^K c_k} \end{aligned}$$

and

$$\begin{aligned} R_{\boldsymbol{\theta}'}(\mathbf{c}) &= \sum_{t=1}^{\ell-1} (w_t - w_{t-1}) e^{\sum_{k=t}^K c_k} \\ &\quad + (w_{\ell+1} - w_{\ell-1}) e^{\sum_{k=\ell}^K c_k} \\ &\quad + (w_{\ell} - w_{\ell+1}) e^{c_{\ell} + \sum_{k=\ell+2}^K c_k} \\ &\quad + (w_{\ell+2} - w_{\ell}) e^{\sum_{k=\ell+2}^K c_k} \\ &\quad + \sum_{t=\ell+2}^K (w_{t+1} - w_t) e^{\sum_{k=t+1}^K c_k} \end{aligned}$$

We remark that, the difference  $R'(\mathbf{c}) - R(\mathbf{c})$  makes the two summation terms in both the head and tail (if either exists) disappear. See (11) below.

$$\begin{aligned} &R_{\boldsymbol{\theta}'}(\mathbf{c}) - R_{\boldsymbol{\theta}}(\mathbf{c}) \\ &= (w_{\ell+1} - w_{\ell-1}) e^{\sum_{k=\ell}^K c_k} + (w_{\ell} - w_{\ell+1}) e^{c_{\ell} + \sum_{k=\ell+2}^K c_k} \\ &\quad + (w_{\ell+2} - w_{\ell}) e^{\sum_{k=\ell+2}^K c_k} - (w_{\ell} - w_{\ell-1}) e^{\sum_{k=\ell}^K c_k} \\ &\quad - (w_{\ell+1} - w_{\ell}) e^{\sum_{k=\ell+1}^K c_k} - (w_{\ell+2} - w_{\ell+1}) e^{\sum_{k=\ell+2}^K c_k} \\ &= e^{\sum_{k=\ell}^K c_k} \{ (w_{\ell+1} - w_{\ell-1}) - (w_{\ell} - w_{\ell-1}) \} \\ &\quad + e^{\sum_{k=\ell+2}^K c_k} \{ (w_{\ell} - w_{\ell+1}) e^{c_{\ell}} - (w_{\ell+1} - w_{\ell}) e^{c_{\ell+1}} \} \\ &\quad + e^{\sum_{k=\ell+2}^K c_k} \{ (w_{\ell+2} - w_{\ell}) - (w_{\ell+2} - w_{\ell+1}) \} \\ &= e^{\sum_{k=\ell}^K c_k} (w_{\ell+1} - w_{\ell}) + e^{\sum_{k=\ell+2}^K c_k} (w_{\ell+1} - w_{\ell}) \\ &\quad + e^{\sum_{k=\ell+2}^K c_k} (w_{\ell+1} - w_{\ell}) (-e^{c_{\ell}} - e^{c_{\ell+1}}) \\ &= (w_{\ell+1} - w_{\ell}) \left\{ e^{\sum_{k=\ell}^K c_k} - e^{c_{\ell} + \sum_{k=\ell+2}^K c_k} \right. \\ &\quad \left. - e^{\sum_{k=\ell+1}^K c_k} + e^{\sum_{k=\ell+2}^K c_k} \right\} \\ &= (w_{\ell+1} - w_{\ell}) e^{\sum_{k=\ell+2}^K c_k} \{ e^{c_{\ell} + c_{\ell+1}} - e^{c_{\ell}} - e^{c_{\ell+1}} + 1 \} \\ &= (w_{\ell+1} - w_{\ell}) e^{\sum_{k=\ell+2}^K c_k} (e^{c_{\ell}} - 1)(e^{c_{\ell+1}} - 1) \quad (11) \end{aligned}$$

In the result of (11), because  $w_{\ell} > w_{\ell+1}$  and  $c_{\ell} \geq 0$  ( $\ell = 1, 2, \dots, K$ ), we conclude

$$R_{\boldsymbol{\theta}'}(\mathbf{c}) \leq R_{\boldsymbol{\theta}}(\mathbf{c}), \text{ for any } \mathbf{c} \geq \mathbf{0}.$$

As a result,

$$\{\mathbf{c} : R_{\boldsymbol{\theta}}(\mathbf{c}) \leq p\} \subseteq \{\mathbf{c} : R_{\boldsymbol{\theta}'}(\mathbf{c}) \leq p\} \quad (12)$$

The result in (12) shows that, for two adjacent UEs  $\ell$  and  $\ell + 1$  with  $w_{\ell} > w_{\ell+1}$ , swapping the order of the two UEs

enlarges the pseudo rate region. We therefore conclude that the correct decoding order yields the largest rate region, namely,

$$\{c : R_{\theta}(c) \leq p\} \subseteq \{c : R_{\theta^*}(c) \leq p\}$$

and, for any  $c \geq 0$ ,

$$R_{\theta^*}(c) \leq R_{\theta}(c).$$

The above holds for any  $\theta \in \mathcal{B}$ , and the theorem follows.  $\square$

### B. Convergence and Optimality of Fixed-Point Algorithm for Load Coupling with NOMA

In this section, we investigate the convergence of the approach for solving (5) as outlined in Section III, without any restriction/limitation. We first re-define the single-cell problem in (6) in Section III, by taking into consideration the dependency between decoding order and interference.

$$f_i(\rho_{-i}) = \min_{q, x, w, \theta} \rho_i \text{ s.t. (5b)–(5h) of cell } i \quad (13)$$

We remark that, though  $\theta$  is variable in (13), it will induce the correct decoding order  $\theta^*$  by constraints (5f)–(5h), because here  $\rho_{-i}$  and hence interference is known. Therefore,  $\theta$  is determined for any given  $\rho_{-i}$  in (13). However, we do not eliminate the  $\theta$  variables from (13), because even though  $\theta^*$  is directly induced by  $\rho_{-i}$ , the latter is variable in the fixed-point iterations, for which we will prove the convergence and optimality.

We first prove Lemma 1 below. In the lemma, the definition of  $c_{ju}$  follows that in (3), however the dependency of  $c_{ju}$  as a function of  $w_j$  is now made explicit.

**Lemma 1.** *Given non-negative  $w_j$ , the inequalities below hold for any  $\alpha > 1$ .*

$$\frac{1}{\alpha} c_{ju}(w_j) < c_{ju}(\alpha w_j)$$

*Proof.* Since  $1/c_{ju}(w_j)$  is strictly concave in  $\rho_{-i}$ , we have

$$\frac{1}{c_{ju}(\alpha w_j)} < \frac{\alpha}{c_{ju}(w_j)} \Rightarrow \frac{1}{\alpha} c_{ju}(w_j) < c_{ju}(\alpha w_j)$$

$\square$

We use  $f_i(\rho_{-i}, \theta)$  to represent the optimization problem defined in (13) under any given  $\theta$  ( $\theta \in \mathcal{B}$ ). Mathematically:

$$f_i(\rho_{-i}, \theta) = \min_{q, x, w} \rho_i \text{ s.t. (5b)–(5e) of cell } i \quad (14)$$

We remark that by variable substitution as in Section IV-A, one has a reformulation of  $f_i(\rho_{-i}, \theta)$ , with  $q$  replaced by  $c$ :

$$f_i(\rho_{-i}, \theta) = \min_{c, x, w} \rho_i \quad (15a)$$

$$\text{s.t. } R_{\theta}(c, w) \leq p_i \quad (15b)$$

(5c) and (5e) of cell  $i$

Note that the single-cell optimization problem above always has a solution, because the problem is to minimize resource usage subject to given demand and interference, and there is no

upper limit imposed for resource usage. As a result, function  $f_i(\rho_{-i}, \theta)$  is well defined.

**Lemma 2.** *For any given  $\theta$  ( $\theta \in \mathcal{B}$ ),  $f_i(\rho_{-i}, \theta)$  is an SIF of  $\rho_{-i}$  ( $\rho_{-i} \geq 0$ ).*

*Proof.* (Monotonicity) Consider any  $f_i(\rho_{-i}, \theta)$  ( $\theta \in \mathcal{B}$ ), and (14). For any  $\rho_{-i}$  and  $\rho'_{-i}$  with  $\rho'_{-i} \leq \rho_{-i}$ , we have  $w_j(\rho_{-i}) \geq w_j(\rho'_{-i})$  ( $j \in \mathcal{U}_i$ ). Therefore  $c_{ju}(\rho_{-i}) \leq c_{ju}(\rho'_{-i})$ . Replacing  $c_{ju}(\rho_{-i})$  by  $c_{ju}(\rho'_{-i})$  leads to a relaxation on the constraints (5b), resulting in lower objective value. We then conclude  $f_i(\rho'_{-i}, \theta) \leq f_i(\rho_{-i}, \theta)$  for any  $\theta \in \mathcal{B}$ .

(Scalability) Denote the value of  $f_i(\rho_{-i}, \theta)$  by  $\rho_i''$ , i.e.  $\rho_i'' = f_i(\rho_{-i}, \theta)$ . Denote the optimal solution of  $f_i(\rho_{-i}, \theta)$  by  $\langle q'', x'', w'' \rangle$ . Under  $\rho_{-i}$ , consider the following minimization problem. Denote its optimal objective value by  $z$ .

$$z = \min_{q, w, x} \rho_i \quad (16a)$$

$$\text{s.t. } \frac{1}{\alpha} \sum_{u \in \mathcal{U}_j} c_{ju}(q, w_j) x_u \geq d_j, j \in \mathcal{J}_i \quad (16b)$$

(5c)–(5e) of cell  $i$

It is straightforward to verify that  $\langle q'', w'', \alpha x'' \rangle$  is feasible to (16), with the objective value equaling  $\alpha f_i(\rho_{-i}, \theta)$ . We conclude that the optimum of (16) is no higher than  $\alpha f_i(\rho_{-i}, \theta)$ . Namely, we have

$$z \leq \alpha f_i(\rho_{-i}, \theta). \quad (17)$$

For  $f_i(\alpha \rho_{-i}, \theta)$ , the corresponding formulation is as follows, where we remark that multiplying  $\alpha$  on  $\rho_{-i}$  is equivalent to performing the multiplication on  $w_j$  for all  $j \in \mathcal{J}_i$ .

$$f_i(\alpha \rho_{-i}, \theta) = \min_{q, w, x} \rho_i \quad (18a)$$

$$\text{s.t. } \sum_{u \in \mathcal{U}_j} c_{ju}(q, \alpha w_j) x_u \geq d_j, j \in \mathcal{J}_i \quad (18b)$$

(5c)–(5e) of cell  $i$

Note that (18) differs from (16) only in (18b), and (16b) is equality at optimum. By Lemma 1, for any solution of (16), using it for (18) makes (18b) an inequality. Therefore, (18) has a better optimum than (16), i.e.

$$f_i(\alpha \rho_{-i}, \theta) < z. \quad (19)$$

By (17) and (19),  $f_i(\alpha \rho_{-i}, \theta) < \alpha f_i(\rho_{-i}, \theta)$  holds.  $\square$

**Lemma 3.** *The NOMA decoding order  $\theta^*$  is optimal to  $\min_{\theta \in \mathcal{B}} f_i(\rho_{-i}, \theta)$  ( $i \in \mathcal{I}$ ), i.e.,*

$$f_i(\rho_{-i}, \theta^*) = \min_{\theta \in \mathcal{B}} f_i(\rho_{-i}, \theta), i \in \mathcal{I}.$$

*Proof.* Consider any cell  $i$  ( $i \in \mathcal{I}$ ) and any decoding order  $\theta$  other than the correct one. By Theorem 1, under fixed  $c$  and  $w$ , replacing  $R_{\theta}(c, w)$  by  $R_{\theta^*}(c, w)$  makes the constraint (15b) remain satisfied (or relaxed if  $R_{\theta^*}(c, w) < R_{\theta}(c, w)$ ), such that one will not get a worse objective value under the correct decoding order. Hence, we conclude that, at the optimum of  $\min_{\theta \in \mathcal{B}} f_i(\rho_{-i}, \theta)$ ,  $\theta$  is (or can be replaced by)  $\theta^*$ . Hence  $\theta^* \in \arg \min_{\theta \in \mathcal{B}} f_i(\rho_{-i}, \theta)$ .  $\square$

By Lemma 3, the minimum of  $f_i$  for any cell and user group is achieved by using the NOMA decoding order  $\theta^*$ . In other words, in any fixed-point iteration, using  $\theta^*$  that is induced by the interference in that iteration, does not cause any loss of optimality in the iteration's output.

We then prove Theorem 2 below.

**Theorem 2.** *The function  $f_i(\rho_{-i})$  ( $i \in \mathcal{I}$ ) in (13) is SIF.*

*Proof.* First, note that  $f_i(\rho_{-i}) = f_i(\rho_{-i}, \theta^*)$ , by the definitions of the two functions  $f_i(\rho_{-i})$  and  $f_i(\rho_{-i}, \theta)$ , and  $\theta^*$ . Second, by Lemma 3, we have  $f_i(\rho_{-i}, \theta^*) = \min_{\theta \in \mathcal{B}} f_i(\rho_{-i}, \theta)$ . Therefore, we conclude  $f_i(\rho_{-i}) = \min_{\theta \in \mathcal{B}} f_i(\rho_{-i}, \theta)$ . The theorem follows then from the fact that the minimum of finitely many SIFs is also an SIF [49].  $\square$

The following corollary shows an algorithmic framework for optimally solving problem (5). Briefly, one only needs to apply fixed-point iterations on all  $f_i$  ( $i \in \mathcal{I}$ ) to reach optimality. Given cell loads  $\rho_{-i}$ , evaluating  $f_i(\rho_{-i})$  ( $i \in \mathcal{I}$ ) submits to a single-cell load minimization problem.

**Corollary 1.** *Assume that problem (5) has a solution, then the iterations  $\rho^{(k+1)} = \mathbf{f}(\rho^{(k)})$ , with arbitrary starting point  $\rho^{(0)}$  ( $\rho^{(0)} \geq \mathbf{0}$ ), converge to a unique fixed-point  $\rho^*$ , such that  $\rho^* = \mathbf{f}(\rho^*)$ . Let  $\mathbf{q}^*, \mathbf{x}^*, \mathbf{w}^*, \theta^*$  be the solution obtained by solving the problems  $f_i(\rho_{-i}^*)$  for all  $i \in \mathcal{I}$ . Then for problem (5), we have*

- 1) *The optimal solution is  $\mathbf{q}^*, \mathbf{x}^*, \mathbf{w}^*, \theta^*$ .*
- 2) *The optimal objective value is  $F(\rho_1^*, \rho_2^*, \dots, \rho_n^*)$ .*

The proof of Corollary 1 can be straightforwardly derived based on Theorem 2. One can refer to [1, Theorem 3] or [2, Theorem 6] for more details.

By Corollary 1, (5) has a unique solution  $\rho^* = [\rho_1^*, \dots, \rho_n^*]$ . Therefore, with post-processing, one can determine if  $\rho^*$  is within the resource limit, i.e., if  $\rho_i^* \leq \bar{\rho}$ ,  $i \in \mathcal{I}$ ; the violation of the constraint for any cell means the problem is infeasible.

## V. DISCUSSION

This section discusses the potential application of our derived results in Section IV along three dimensions: *problem formulation, tractability, and optimality*.

### A. Decoding Order Constraints

It is worth noting that constraints (5f) are redundant for (5). Consider the formulation below.

$$\min_{\mathbf{q}, \mathbf{x}, \rho, \mathbf{w}, \theta \geq \mathbf{0}} F(\rho_1, \rho_2, \dots, \rho_n) \text{ s.t. (5b)–(5e), (5g), and (5h)}$$

Theorem 1 along with the analysis in Section IV indeed reveals that at its optimum,  $\theta = \theta^*$ . Namely, for any  $\theta_{h_j}$  at the optimum, if  $\theta_{h_j} = 1$ , we must have  $w_h \leq w_j$ , meaning that  $\theta_{h_j}$  satisfies  $\theta_{h_j} \geq \min\{1, w_j - w_h\}$ . Hence the non-linear constraints (5f) are redundant and can be removed from the formulation.

### B. Tractability of (5)

We remark that even though (5) is for multi-cell scenarios, the difficulty indeed lies in its corresponding single-cell load minimization problems, i.e., (13). By Lemma 3 we reach the optimum at  $\theta^*$ . Once  $f_i(\rho_{-i}, \theta^*)$  can be solved to optimality, then as pointed out by Corollary 1, the optimum of (5) can be straightforwardly obtained. There are some special cases of (14) that submit to a polynomial-time solution, briefly discussed below.

If the power allocation  $\mathbf{q}$  is fixed, then the single-cell load minimization problem (6) is a linear programming problem in  $\mathbf{x}$  and  $\mathbf{w}$  [1]. We remark that (14) can be reformulated to (15) by using the successive rule in Section IV-A. As the second case, if the demand on each user group is given, then variable  $\mathbf{x}$  can be eliminated, and (15) is a convex programming formulation<sup>2</sup> of  $\mathbf{c}$  and  $\mathbf{w}$  [50].

Consider another case where the number of UEs in each group is no more than two (i.e.  $|u| \leq 2$  for all  $u \in \mathcal{U}$ ,  $i \in \mathcal{I}$ ), and there is no overlapping UE for any two selected groups. Then (5) can be solved optimally within polynomial time by combinatorial optimization [2]. The basic idea is to bring the single-cell load optimization down to the group level, and then prove that the optimal group selection amounts to solving a maximum matching problem.

For the general case of (14), whether it is tractable or not, remains open, suggesting future research to be done along this direction.

### C. A Comment on [1], [2]

In [1], [2], the proposed solution has guaranteed convergence if some restrictions, [1, Lemma 1] and [2, Lemma 1], are imposed. The results derived in this technical note provide a complementary theoretical insight, namely, the restrictions can be dropped without any loss of optimality or convergence.

## VI. NUMERICAL RESULTS

In this section, we provide performance comparison of OMA and NOMA, as well as numerical validation of our theoretical findings. We use a cellular network of 19 cells, with wrap-around for eliminating edge effects. The simulation settings are given in Table I.

Table I  
SIMULATION PARAMETERS.

Parameter	Value
Cell radius	500 m
Carrier frequency	2 GHz
Total bandwidth	20 MHz
Cell load limit $\bar{\rho}$	1.0
Path loss model	COST-231-HATA
Shadowing (Log-normal)	6 dB standard deviation
Fading	Rayleigh flat fading
Noise power spectral density	-173 dBm/Hz
RB power $p_i$ ( $i \in \mathcal{I}$ )	800 mW
Convergence tolerance ( $\epsilon$ )	$10^{-4}$

<sup>2</sup>We remark that the convexity of constraints (15b) holds if  $\theta$  is set to be the correct decoding order). By Lemma 3, we know that this is the only case that needs to be taken into account.

The sum load minimization problem, i.e.,  $F(\rho) = \sum_{i \in \mathcal{I}} \rho_i$  in formulation (5), can be used to examine the maximum throughput supported, for uniform user demand. A given demand level (of all users) can be supported, if and only if load minimization leads to load levels that are all within the load limit. Hence the maximum throughput can be computed by solving (5) repeatedly with a bi-section search on the demand level. For this experiment, there are 30 UEs randomly distributed inside each cell. Each user group  $u$  contains two UEs. We remark that both OMA and NOMA are solved to optimality. In OMA, the optimum is obtained by using the method in [15]. In NOMA, we use the algorithm proposed in [2]. However, the constraint imposed by [2, Lemma 1] on the candidate user groups is dropped, and, by our theoretical results, there is no loss of global optimality.

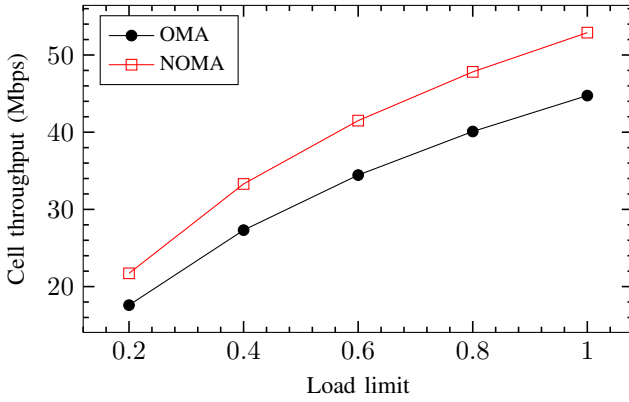


Figure 1. Cell throughput (in Mbps) in function of load limit.

Figure 1 shows the performance in terms of the throughput (in Mbps) per cell, for various levels of the cell load limit. We remark that in the derivations in the previous sections, the data is in nats, merely to simplify the mathematical expressions. Here, for convenience, we show the results in bits. Note that all users of a cell, including those located at cell edge, are provided with the same data rate. From Figure 1, NOMA leads to considerably higher throughput than OMA, while consuming the same amount of resource. The performance improvement is about 20% or higher. Moreover, even though the absolute difference increases with the cell load limit, the relative difference is in fact higher when the load limit is low, that is, NOMA offers more performance gain when the use of resource is more constrained.

It should be pointed out that not all cells are able to utilize 100% of the resource simultaneously to maximize the throughput. To clarify further this aspect, in Figure 2 we show the individual cell load levels at the maximum achievable OMA throughput, with load limit being equal to one, i.e., the load levels of OMA and NOMA corresponding the right-end of the two curves in Figure 1. Indeed, for OMA, one can observe that one cell has reached the limit, whereas the other cells still have spare resource. However, these cells are not able to consume the spare resource, because doing so would lead to higher interference, as captured by the load-coupling model, overloading the cell that currently is fully loaded. While delivering the same throughput as OMA, by

NOMA the load is less than 70% in all cells. As none of the cells has exhausted its resource, additional throughput can be offered.

As our next of numerical study, we consider the number of users that can be supported per cell by OMA and NOMA, for various demand levels. To this end, for each demand level, we run 1,000 realizations for different numbers of users per cell, and record whether or not OMA and NOMA can simultaneously support all users. The results are then collected to generate the cumulative density function (CDF) shown in Figure 3. For the lowest demand used, OMA can support approximately 30 users in every cell with 90% probability. For NOMA, the corresponding number is close to 45 users, representing an increase of 50%. Similar amount of improvement is observed for the higher demand levels. Moreover, for all the demand levels, when the number of users per cell has reached the level such that the probability of supporting all of them by OMA is virtually zero, NOMA still has approximately 40% probability of supporting this number and higher. Hence the performance enhancement, in terms of the number of users that can be accommodated by the network, is significant.

Next, we make a comparison of spectral efficiency (in bps/Hz) of OMA and NOMA, with respect to the proportion of cell-edge users. Cell-edge users are those such that the distance to the home base station is at least 80% of the cell radius. The results are provided in Figure 4. Again, by our theoretical findings, the numerical results here represent the achievable performance, and hence the comparison is accurate. From the figure, the impact of cell-edge users on performance is very apparent. Specifically, when there is no cell-edge user at all, the spectral efficiency is 30% higher for NOMA. The spectral efficiency drops then quickly with respect to the proportion of cell-edge users, and the improvement offered by NOMA has a diminishing trend<sup>3</sup>. That is, much less improvement can be expected from NOMA for scenarios where many users are at cell edge.

In Figure 5, we show the convergence as well as the convergence rate of fixed-point iterations of function  $f(\rho)$ . The theoretical guarantee of convergence, as stated earlier in this note, is indeed observed. Moreover, high accuracy of the network load can be reached after very few iterations on  $f(\rho)$ , and the algorithm converges slightly faster for higher user demand.

To summarize, NOMA provides considerable throughput gain over OMA, the underlying reason is that, for the same demand level, NOMA requires significantly less resource usage in all cells, and the spare resource can be utilized for more throughput. For the same reason, NOMA exhibits significant improvement in the number of users that can be supported. However, the amount of performance improvement to expect is tied to the proportion of cell-edge users. The simulation study also confirms the correctness of our theoretical analysis of convergence guarantee of the fixed-point algorithm.

<sup>3</sup>Even though in numbers, NOMA still delivered more than 10% higher efficiency with 20% cell-edge users.

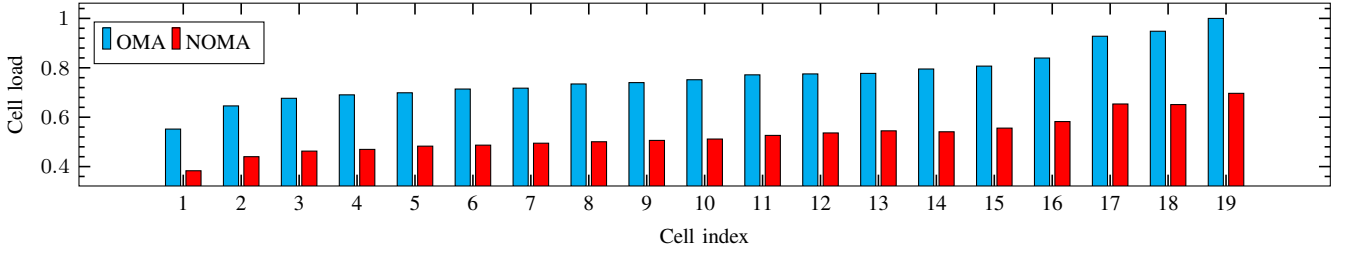


Figure 2. Cell load levels sorted in ascending order for NOMA, with load limit 1.0.

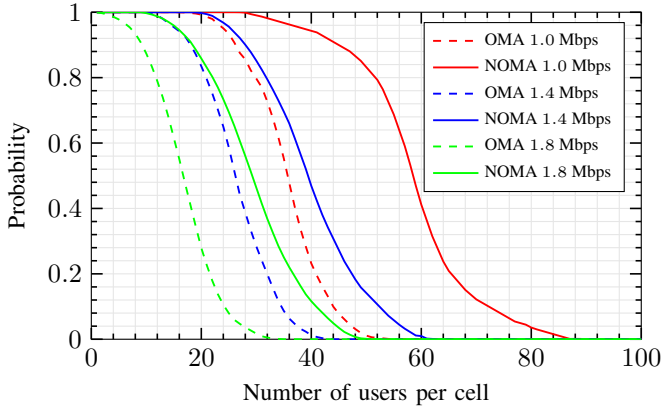


Figure 3. This figure illustrates the cumulative density function of having all users supported in every cell. The demand values in the legend are for each user.

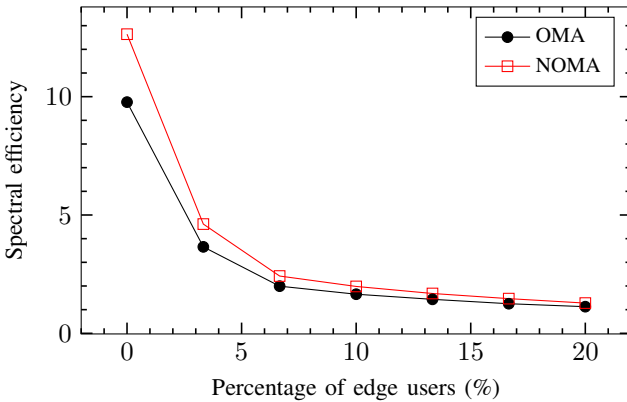


Figure 4. This figure illustrates the spectral efficiency as function of the proportion of cell edge users.

## VII. CONCLUSION

This technical note has addressed the convergence and optimality of an algorithmic framework for solving a class of optimization problems in multi-cell NOMA networks. The note proved that the correct decoding order corresponds to the largest region. Then, results for convergence and optimality, with variable decoding order in the iterative process, are formally established. The note has also discussed the tractability of multi-cell optimization with load coupling, and reveals that solving the single-cell problem is the key in terms of tractability.

We remark that for contraction mapping, the convergence

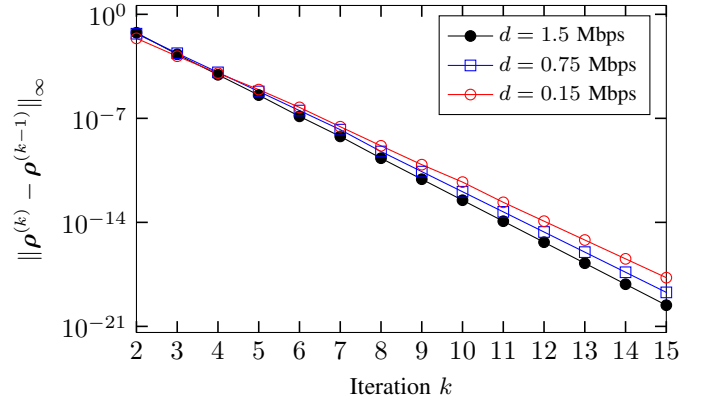


Figure 5. This figure shows the norm  $\|\cdot\|_\infty$  in function of iteration  $k$  ( $k \geq 2$ ), under the uniform demand settings of  $d = 1.5$ ,  $0.75$ , and  $0.15$  Mbps for each user, respectively, with 30 users per cell.

rate of fixed-point iterations is linear, see [51]. However for general SIFs the convergence can be sub-linear. Hence, an interesting topic of further study is to examine conditions under which the SIF for NOMA optimization falls within the domain of contraction mapping, to shed light on the convergence rate in addition to the convergence results proved in the current paper.

As was discussed in Section I, in NOMA it is assumed that the data rate used for a user equals what is permitted by the SINR. Suppose the rate is also subject to selection, such that it can be set to be lower than the SINR-rate, in order to enable interference cancellation. Although such a scheme is not part of the original NOMA, combining this aspect with user grouping and power split of NOMA opens up a new research line for future work.

A further line of our future research consists in accounting for the impact of imperfect channel estimation on NOMA performance, as well as means mitigating the problem of propagation error. The study amounts to incorporating these aspects in the system model, and investigating the resulting multi-cell NOMA optimization problem, for which the results of the current paper will be used for benchmarking purposes.

## ACKNOWLEDGMENT

We would like to thank the reviewers and the editor for the valuable comments that have enabled us to improve the paper, as well as the inspirations thanks to the comments on future work (e.g., combining rate selection with NOMA is inspired by a comment of Reviewer 3.)

## REFERENCES

- [1] L. You, L. Lei, D. Yuan, S. Sun, S. Chatzinotas, and B. Ottersten, "A framework for optimizing multi-cell noma: Delivering demand with less resource," in *2017 IEEE GLOBECOM*, Dec 2017, pp. 1–7.
- [2] L. You, D. Yuan, L. Lei, S. Sun, S. Chatzinotas, and B. Ottersten, "Resource optimization with load coupling in multi-cell noma," *IEEE Transactions on Wireless Communications*, vol. 17, no. 7, pp. 4735–4749, July 2018.
- [3] Y. Saito, A. Benjebbour, Y. Kishiyama, and T. Nakamura, "System-level performance evaluation of downlink non-orthogonal multiple access (NOMA)," in *2013 IEEE PIMRC*, 2013, pp. 611–615.
- [4] M. S. Ali, H. Tabassum, and E. Hossain, "Dynamic user clustering and power allocation for uplink and downlink non-orthogonal multiple access (NOMA) systems," *IEEE Access*, vol. 4, pp. 6325–6343, 2016.
- [5] J. Kang and I. Kim, "Optimal user grouping for downlink NOMA," *IEEE Wireless Communications Letters*, vol. 7, no. 5, pp. 724–727, Oct 2018.
- [6] L. Lei, D. Yuan, C. K. Ho, and S. Sun, "Power and channel allocation for non-orthogonal multiple access in 5G systems: Tractability and computation," *IEEE Transactions on Wireless Communications*, vol. 15, no. 12, pp. 8580–8594, 2016.
- [7] J. Kim, J. Koh, J. Kang, K. Lee, and J. Kang, "Design of user clustering and precoding for downlink non-orthogonal multiple access (NOMA)," in *2015 IEEE MILCOM*, 2015, pp. 1170–1175.
- [8] Z. Ding, P. Fan, and H. V. Poor, "Impact of user pairing on 5G nonorthogonal multiple-access downlink transmissions," *IEEE Transactions on Vehicular Technology*, vol. 65, no. 8, pp. 6010–6023, 2016.
- [9] Z. Ding, Y. Liu, J. Choi, Q. Sun, M. Elkashlan, C. L. I, and H. V. Poor, "Application of non-orthogonal multiple access in LTE and 5G networks," *IEEE Communications Magazine*, vol. 55, no. 2, pp. 185–191, 2017.
- [10] S. M. R. Islam, N. Avazov, O. A. Dobre, and K. S. Kwak, "Power-domain non-orthogonal multiple access (NOMA) in 5G systems: Potentials and challenges," *IEEE Communications Surveys Tutorials*, vol. 19, no. 2, pp. 721–742, 2017.
- [11] W. Shin, M. Vaezi, B. Lee, D. J. Love, J. Lee, and H. V. Poor, "Non-orthogonal multiple access in multi-cell networks: Theory, performance, and practical challenges," *arXiv.org*, 2016. [Online]. Available: <https://arxiv.org/pdf/1611.01607.pdf>
- [12] L. You and D. Yuan, "Joint CoMP-cell selection and resource allocation in fronthaul-constrained C-RAN," in *2017 WiOpt Workshop*, 2017, pp. 1–6.
- [13] L. Lei, D. Yuan, C. K. Ho, and S. Sun, "Optimal cell clustering and activation for energy saving in load-coupled wireless networks," *IEEE Transactions on Wireless Communications*, vol. 14, no. 11, pp. 6150–6163, 2015.
- [14] I. Viering, M. Döttling, and A. Lobinger, "A mathematical perspective of self-optimizing wireless networks," in *2009 IEEE ICC*, 2009, pp. 1–6.
- [15] I. Siomina and D. Yuan, "Analysis of cell load coupling for LTE network planning and optimization," *IEEE Transactions on Wireless Communications*, vol. 11, no. 6, pp. 2287–2297, 2012.
- [16] A. J. Fehske, I. Viering, J. Voigt, C. Sartori, S. Redana, and G. P. Fettweis, "Small-cell self-organizing wireless networks," *Proceedings of the IEEE*, vol. 102, no. 3, pp. 334–350, 2014.
- [17] L. You, D. Yuan, N. Pappas, and P. Värbrand, "Energy-aware wireless relay selection in load-coupled OFDMA cellular networks," *IEEE Communications Letters*, vol. 21, no. 1, pp. 144–147, 2017.
- [18] L. You and D. Yuan, "Load optimization with user association in cooperative and load-coupled LTE networks," *IEEE Transactions on Wireless Communications*, vol. 16, no. 5, pp. 3218–3231, 2017.
- [19] I. Siomina, A. Furusk, and G. Fodor, "A mathematical framework for statistical QoS and capacity studies in OFDM networks," in *2009 IEEE PIMRC*, 2009, pp. 2772–2776.
- [20] K. Majewski and M. Koonert, "Conservative cell load approximation for radio networks with Shannon channels and its application to LTE network planning," in *2010 Sixth Advanced International Conference on Telecommunications*, 2010, pp. 219–225.
- [21] E. Pollakis, R. L. G. Cavalcante, and S. Staczak, "Base station selection for energy efficient network operation with the majorization-minimization algorithm," in *2012 IEEE SPAWC*, 2012, pp. 219–223.
- [22] A. J. Fehske and G. P. Fettweis, "Aggregation of variables in load models for interference-coupled cellular data networks," in *2012 IEEE ICC*, 2012, pp. 5102–5107.
- [23] A. J. Fehske, H. Klessig, J. Voigt, and G. P. Fettweis, "Concurrent load-aware adjustment of user association and antenna tilts in self-organizing radio networks," *IEEE Transactions on Vehicular Technology*, vol. 62, no. 5, pp. 1974–1988, 2013.
- [24] C. K. Ho, D. Yuan, and S. Sun, "Data offloading in load coupled networks: A utility maximization framework," *IEEE Transactions on Wireless Communications*, vol. 13, no. 4, pp. 1921–1931, April 2014.
- [25] R. L. G. Cavalcante, S. Staczak, M. Schubert, A. Eisenblatter, and U. Tuerke, "Toward energy-efficient 5G wireless communications technologies: Tools for decoupling the scaling of networks from the growth of operating power," *IEEE Signal Processing Magazine*, vol. 31, no. 6, pp. 24–34, 2014.
- [26] S. Tombaz, S. w. Han, K. W. Sung, and J. Zander, "Energy efficient network deployment with cell DTX," *IEEE Communications Letters*, vol. 18, no. 6, pp. 977–980, 2014.
- [27] B. Baszczyszyn, M. Jovanovic, and M. K. Karray, "Performance laws of large heterogeneous cellular networks," in *2015 WiOpt*, 2015, pp. 597–604.
- [28] C. K. Ho, D. Yuan, L. Lei, and S. Sun, "Power and load coupling in cellular networks for energy optimization," *IEEE Transactions on Wireless Communications*, vol. 14, no. 1, pp. 509–519, 2015.
- [29] R. L. G. Cavalcante, S. Staczak, J. Zhang, and H. Zhuang, "Low complexity iterative algorithms for power estimation in ultra-dense load coupled networks," *IEEE Transactions on Signal Processing*, vol. 64, no. 22, pp. 6058–6070, 2016.
- [30] H. Klessig, D. Hmann, A. J. Fehske, and G. P. Fettweis, "A performance evaluation framework for interference-coupled cellular data networks," *IEEE Transactions on Wireless Communications*, vol. 15, no. 2, pp. 938–950, 2016.
- [31] R. L. G. Cavalcante, Y. Shen, and S. Staczak, "Elementary properties of positive concave mappings with applications to network planning and optimization," *IEEE Transactions on Signal Processing*, vol. 64, no. 7, pp. 1774–1783, 2016.
- [32] Q. Liao, "Dynamic uplink/downlink resource management in flexible duplex-enabled wireless networks," in *2017 ICC Workshops*, 2017, pp. 625–631.
- [33] R. L. G. Cavalcante, M. Kasparick, and S. Staczak, "Max-min utility optimization in load coupled interference networks," *IEEE Transactions on Wireless Communications*, vol. 16, no. 2, pp. 705–716, 2017.
- [34] D. A. Awan, R. L. G. Cavalcante, and S. Staczak, "A robust machine learning method for cell-load approximation in wireless networks," *arXiv.org*, 2017. [Online]. Available: <http://arxiv.org/abs/1710.09318>
- [35] J. Cui, Y. Liu, Z. Ding, P. Fan, and A. Nallanathan, "Qoe-based resource allocation for multi-cell NOMA networks," *IEEE Transactions on Wireless Communications*, vol. 17, no. 9, pp. 6160–6176, 2018.
- [36] M. S. Elbamby, M. Bennis, W. Saad, M. Debbah, and M. Latva-Aho, "Resource optimization and power allocation in in-band full duplex-enabled non-orthogonal multiple access networks," *IEEE Journal on Selected Areas in Communications*, vol. 35, no. 12, pp. 2860–2873, 2017.
- [37] M. W. Baidas, Z. Bahbahani, and E. Alsusa, "A matching-theoretic approach to user-association and channel assignment in downlink multi-cell NOMA networks," in *2018 Seventh International Conference on Communications and Networking (ComNet)*. IEEE, 2018, pp. 1–8.
- [38] D. P. Kudathanthirige and G. L. A. A. Baduge, "NOMA-aided multi-cell downlink massive MIMO," *IEEE Journal of Selected Topics in Signal Processing*, 2019.
- [39] H. Zeng, X. Zhu, Y. Jiang, Z. Wei, and T. Wang, "A green coordinated multi-cell NOMA system with fuzzy logic based multi-criterion user mode selection and resource allocation," *IEEE Journal of Selected Topics in Signal Processing*, 2019.
- [40] Y. Fu, Y. Chen, and C. W. Sung, "Distributed power control for the downlink of multi-cell NOMA systems," *IEEE Transactions on Wireless Communications*, to appear.
- [41] D. Tse and P. Viswanath, *Fundamentals of Wireless Communication*. Cambridge university press, 2005.
- [42] V. Angelakis, L. Chen, and D. Yuan, "Optimal and collaborative rate selection for interference cancellation in wireless networks," *IEEE Communications Letters*, vol. 15, pp. 819–821, 2011.
- [43] L. Zhou, K. Ruttik, O. Tirkkonen, and R. Berry, "Cell-edge inversion by interference cancellation for downlink cellular systems," in *IEEE International Conference on Communication Systems (ICCS)*, 2014.
- [44] M. Kobayashi, J. Boutros, and G. Caire, "Successive interference cancellation with siso decoding and em channel estimation," *IEEE Journal on Selected Areas in Communications*, vol. 19, no. 8, pp. 1450–1460, August 2001.
- [45] J. Kim, "Mitigating error propagation in successive interference cancellation," *IEICE Transactions on Communications*, vol. 89-B, no. 10, pp. 2956–2960, October 2006.

- [46] R. Fa and R. D. Lamare, "Multi-branch successive interference cancellation for mimo spatial multiplexing systems: Design, analysis and adaptive implementation," *IET Communications*, vol. 5, no. 4, pp. 484–494, March 2011.
- [47] P. Li, R. Fa, and R. D. Lamare, "Multiple feedback successive interference cancellation detection for multiuser mimo systems," *IEEE Transactions on Wireless Communications*, vol. 10, no. 8, pp. 2434–2439, August 2011.
- [48] "IEC 80000-13:2008, quantities and units part 13: Information science and technology," International Electrotechnical Commission, 2008.
- [49] R. D. Yates, "A framework for uplink power control in cellular radio systems," *IEEE Journal on Selected Areas in Communications*, vol. 13, no. 7, pp. 1341–1347, 1995.
- [50] J. Zhu, J. Wang, Y. Huang, S. He, X. You, and L. Yang, "On optimal power allocation for downlink non-orthogonal multiple access systems," *IEEE Journal on Selected Areas in Communications*, vol. 35, no. 12, pp. 2744–2757, 2017.
- [51] H. R. Feyzmahdavian, M. Johansson, and T. Charalambous, "Contractive interference functions and rates of convergence of distributed power control laws," *IEEE Transactions on Wireless Communications*, vol. 11, no. 12, pp. 4494–4502, 2012.